

STUDIES ON LONG-SPAN CONCRETE ARCH BRIDGE FOR CONSTRUCTION AT IKARAJIMA IN JAPAN

Kazuto Kamisakoda^{*}, Hikaru Nakamura[†] and Atsushi Nakamura^{††}

^{*} Civil Engineering Design Division
Kajima Corporation
6-5-30, Akasaka, Minato-ku, Tokyo 107-8502, Japan
e-mail: kamisako@kajima.com, web page: <http://www.kajima.co.jp/>

[†]Department of Civil Engineering
Nagoya University
Furo-cho, Chikusa-ku, Nagoya 464-8603, Japan
e-mail: hikaru@civil.nagoya-u.ac.jp, web page: <http://www.nagoya-u.ac.jp/>

^{††}Civil Engineering Division
Sumitomo Mitsui Construction Co., Ltd.
1-38-1, Chuou, Nakano-ku, Tokyo 164-0011, Japan
e-mail: atnaka@smcon.co.jp, web page: <http://www.smcon.co.jp/>

Key words: Concrete Arch Bridge, Low-Rise Arch, Marine Bridge, High Strength Concrete, Cantilever Erection, Melan, Fiber Model, Eigenvalue Analysis, Time History Response Analysis

Abstract. *Japan Society of Civil Engineers' subcommittee on design methods for long-span concrete arch bridges chaired by Prof. T. Tanabe of Nagoya University developed a trial design of a long-span concrete arch bridge for construction at a particular site. The designed bridge, assumed to be constructed to connect Nagashima (Naga Island) to Ikarajima (Ikara Island) in Kagoshima Prefecture, has an arch span length of 500 m and an arch rise of 40 m and is 17.4 m wide. The trial design indicated that the design strength of arch rib concrete needs to be about 100 MPa or more. The seismic performance of the bridge was verified through static and dynamic checking. Since the bridge is a marine structure, an erection method appropriate for the bridge was considered. The construction period from arch rib construction to bridge surfacing was estimated to be 38 months.*

1 INTRODUCTION

Configuration and erection requirements for an arch bridge vary widely depending on the site conditions. For the purposes of the present study, therefore, a particular erection site was considered. An arch bridge suitable for that particular site was designed, and an erection method for that bridge was determined.

To select an erection site, information on existing bridges of other structural types was collected because such data as road alignment and ground conditions at the sites of those bridges were readily available. The information thus collected was examined to find a site at which a long-span arch bridge can be constructed. As a result, the site of the Ikara Bridge, which connects Nagashima and Ikarajima in the north-western part of Kagoshima Prefecture, was chosen as the site of the imaginary bridge. The Ikara Bridge is a prestressed concrete cable-stayed bridge with a center span length of 260 m, the longest of its kind in Japan .

2 DESIGN ASSUMPTION

2.1 Policy

The most important consideration in selecting a bridge construction site in Japan is the existence of site conditions that make it possible to meet rise requirements. In Japan, it is not uncommon to encounter cases where a span length of 600 m is needed, such as cases where a river has to be crossed or where islands are to be connected by a bridge, but it is not possible to find a site where a rise of about 100 m can be secured.

Consequently, if a deck (i.e., arch-under-deck) bridge with a rise of 100 m were constructed at the site of the Ikara Bridge, the road alignment would need to rise to an excessively high level. So, it was decided to adopt a flat-arch design although such a design differs from the basic trial design model.

As in the trial design procedure for the span length of 600 m, therefore, the erection procedure is determined and seismic performance is checked.

2.2 Design conditions

1) As in the trial design for the span length of 600 m, a typical concrete arch bridge was assumed, and a deck (i.e., arch-under-deck) Lohse fixed-arch bridge design was adopted.

2) Section forces under dead loads are calculated for all falsework construction methods. Section forces under in-plane seismic loads and out-of-plane seismic loads are calculated through three-dimensional elastic frame analysis.

3) The target stress is defined from the allowable stress, and girder depth and member thickness are determined accordingly. In view of such factors as steel reinforcement work, the minimum member thickness for both webs and slabs is 50 cm. If arch rib width is found insufficient as a result of a study of width requirements under out-of-plane seismic loads, an optimum width is determined for both the crown and the springing.

4) The static checking method is used for in-plane and out-of-plane analyses of seismic behavior. The horizontal seismic coefficient is determined taking into account increases in the natural period ($kh = 0.10$ for both in-plane and out-of-plane analysis).

5) Arch abutment configuration is roughly determined from calculated reaction forces by regarding an arch abutment as a structure built directly on a foundation. The allowable limit of subgrade reaction is 1.0 MN/m^2 under design loads and 1.5 MN/m^2 under seismic loads.

6) The bridge will become a flat-arch structure because a deck Lohse bridge design is used. Consequently, large compressive force will occur even if bending moment in the arch rib cross section is reduced by choosing an arch axis appropriately. Thus, because commonly used concrete with a strength of $f_{ck}'=60 \text{ N/mm}^2$ or so does not satisfy the allowable stress requirements, higher strength concrete is used to reduce the self-weight, and the concrete strength required for making it possible to use member cross sections similar to those of the trial design model with a span length of 600 m is determined.

3 TRIAL DESIGN RESULTS

3.1 Structural dimensions

An arch bridge which satisfies the design conditions is shown in Fig. 1.

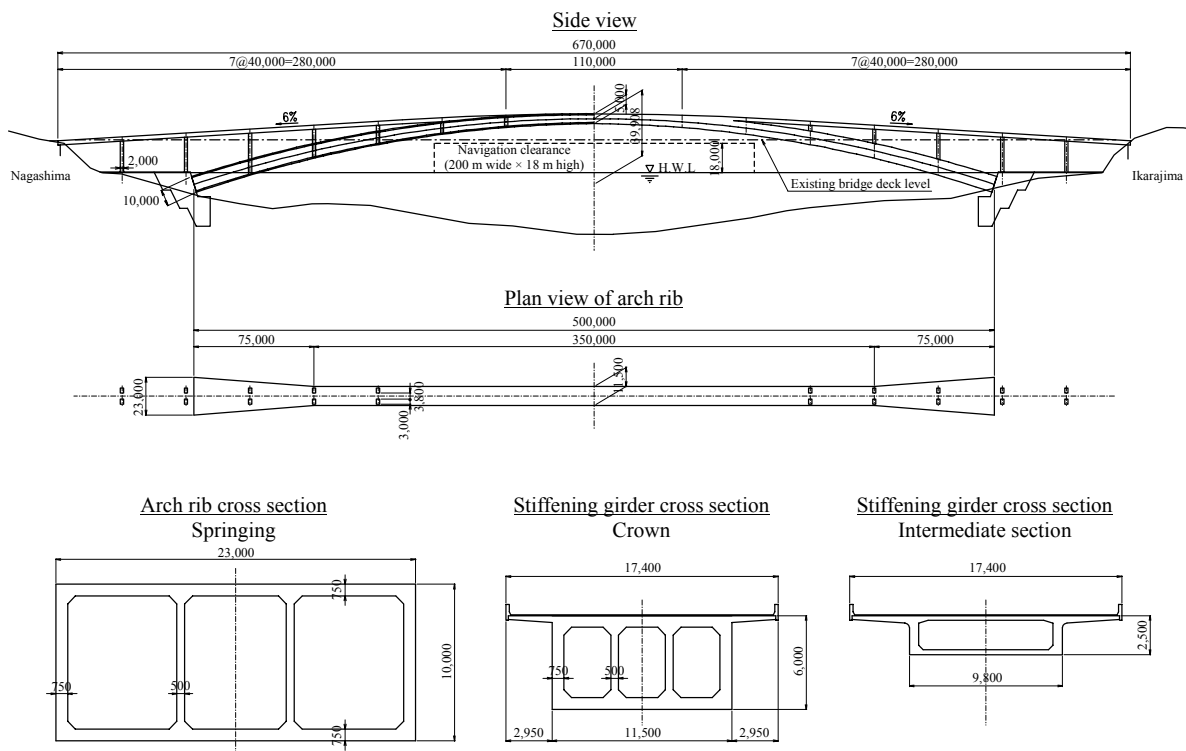


Figure 1: Proposed design of Ikara Bridge (arch bridge)

3.2 Arch rib

Since a concrete stress of about 40 N/mm^2 occurs under the dead load alone even when the arch axis is optimized, the required design strength of concrete is thought to be around 100 to 120 N/mm^2 .

3.3 Arch abutment

Arch abutment configuration is roughly determined from calculated reaction forces by regarding an arch abutment as a structure built directly on a foundation. The height and the width and depth of the arch abutment thus determined are 33 m and 35 m, respectively, and the concrete volume is about 19,160 m³.

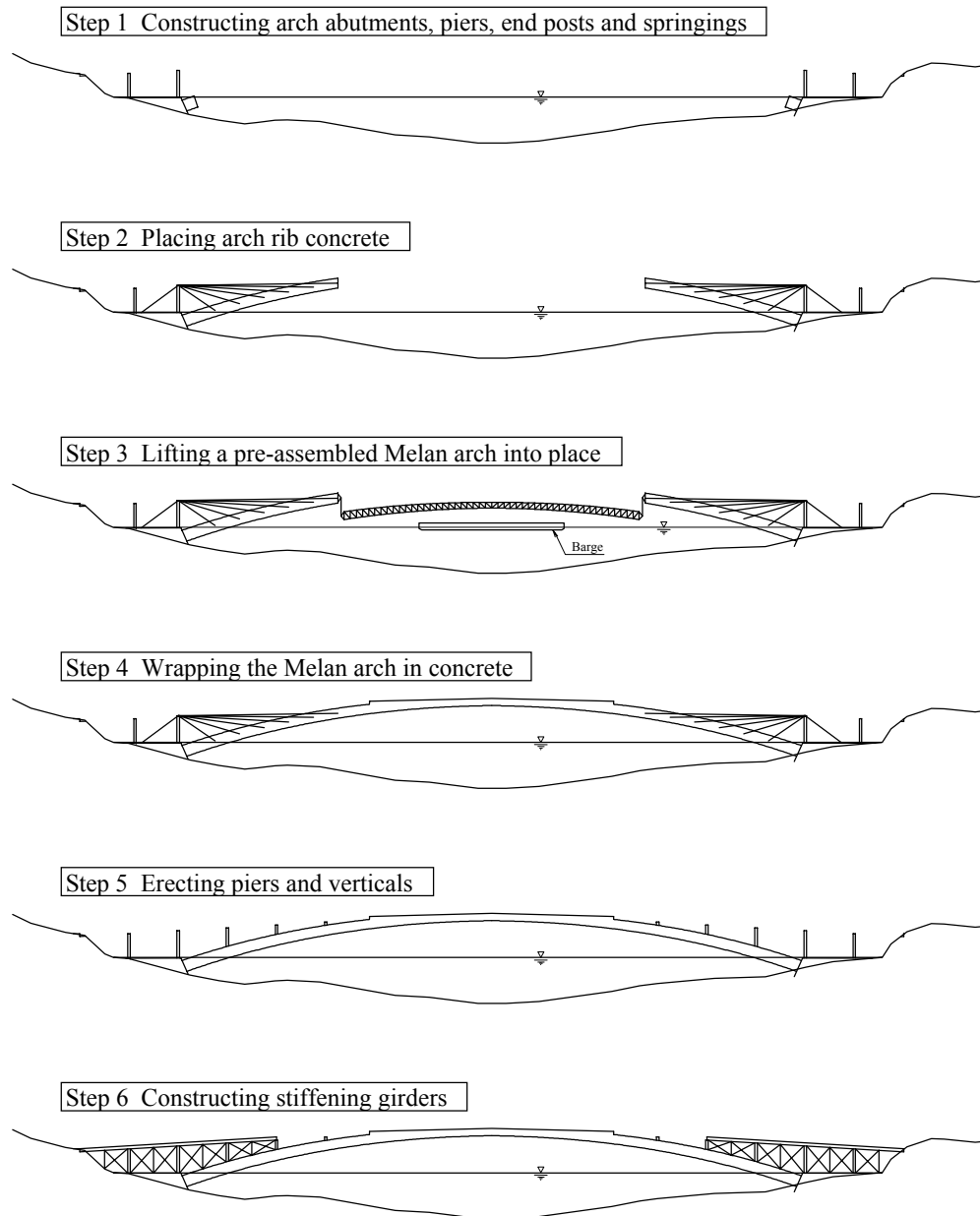


Figure 2: Construction steps

4 PROPOSED ERECTION PLAN

Since the bridge under study is a marine bridge, a pre-assembled Melan arch can be lifted into place from a deck barge. In the proposed erection method, therefore, the bridge sections up to the L/4 points are erected by the cantilever method using stay cables. The remaining section is erected by lifting a pre-assembled Melan arch into place and wrapping the arch in concrete. Fig. 2 illustrates the construction procedure, and Fig. 3 shows the construction schedule.

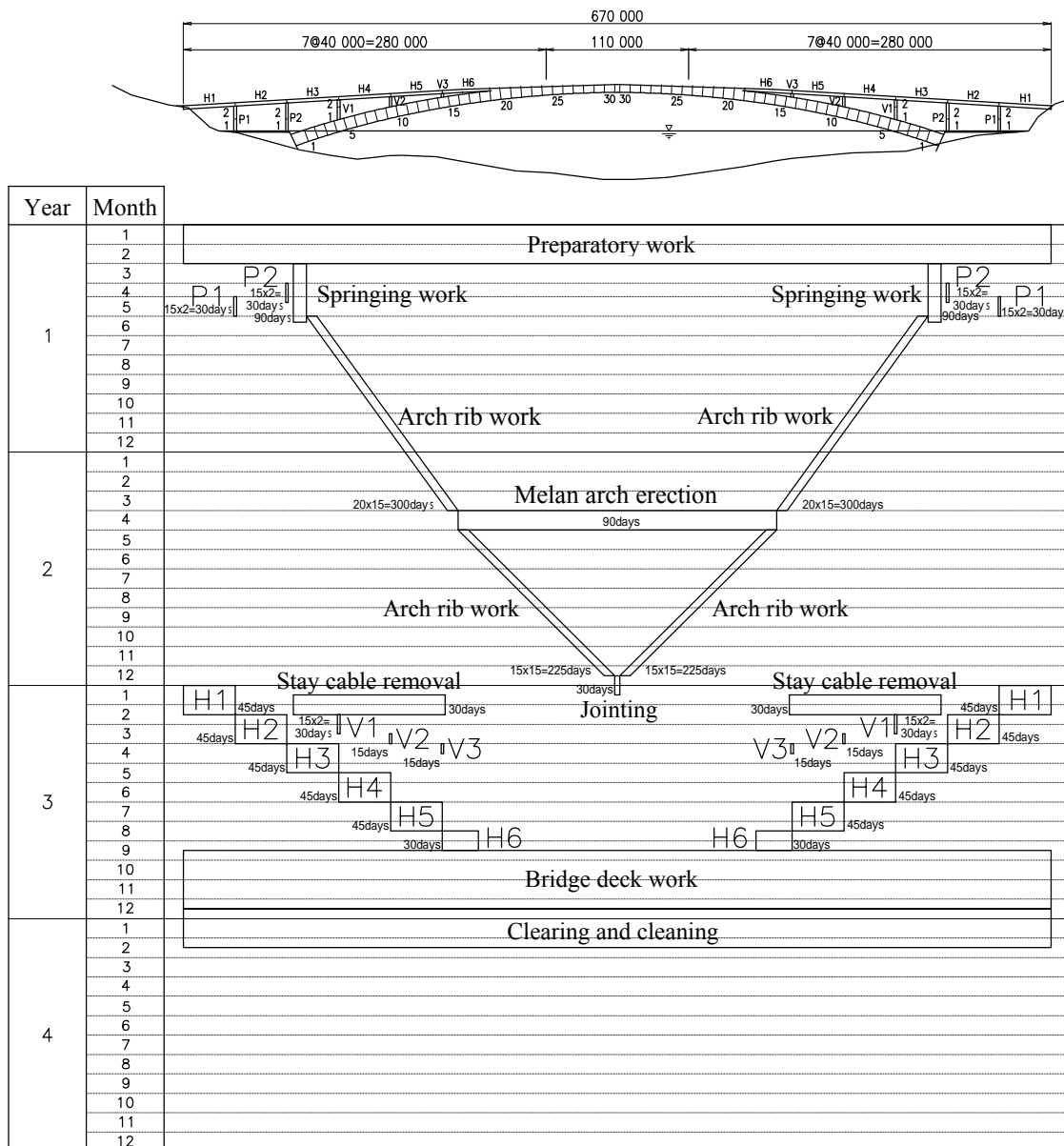


Figure 3: Construction progress schedule

5 CHECK ON PERFORMANCE UNDER NORMAL LOADING

5.1 Checking method

The trial design of the arch bridge was checked by modeling the designed bridge into 61 nodes and 71 elements, using beam elements based on a fiber model that takes geometric nonlinearity into account. Fig. 4 shows the element mesh of the verification model. The geometrical boundary conditions are as follows: both ends of the arch rib are completely fixed; and stiffening girder ends are constrained in the vertical direction and around the bridge axis (girder torsion) and are free in the other directions.

For material modeling, the stress–strain relationships for concrete and steel that reflect hysteresis characteristics were used. A compressive strength f'_c of concrete of 100 N/mm^2 , a strain at compressive strength of $4,000 \mu$, and a strain occurring at the time when stress becomes zero after the compressive strength is reached of $12,000 \mu$ were assumed. Use of SD685 reinforcing bars, a yield strength (both tensile and compressive) of 685 N/mm^2 , and Young's modulus of $2.04 \times 10^5 \text{ N/mm}^2$ were also assumed.

A combination of the displacement control method and the load control method was used. During the loading process, the displacement at point B shown in Fig. 4 was controlled while the vertical load at each node proportional to the dead load vector was controlled. An eigenvalue analysis of the tangential stiffness matrix was conducted at each step to verify structural stability against buckling.

5.2 Results

Performance under normal loading was checked with respect to cross-sectional stress and structural stability. It was assumed that performance requirements under normal loading were satisfied if (1) with respect to cross-sectional stress, neither a stress amounting to $1/3$ or more of the compressive strength of concrete nor a stress amounting to $2/3$ of the yield stress of reinforcing steel occurs and (2) with respect to structural stability, the eigenvalue of the tangential stiffness matrix does not become negative.

Fig. 5 shows the load–vertical displacement relationship at point B shown in Fig. 4, and changes in the eigenvalue. As shown, the designed arch bridge has a load-carrying capacity amounting to about 2.6 times the self-weight. It can be inferred that behavior under normal loading is more or less linear and elastic. It can also be seen that the eigenvalue becomes zero under the maximum load and then becomes negative, but it never becomes negative before the maximum load occurs, indicating that the structural stability requirements under normal loading are satisfied.

Except at the arch springing, stresses in the arch rib cross section are completely compressive, and the

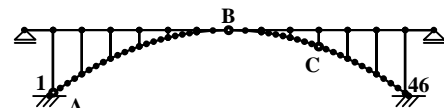


Figure 4: Verification model

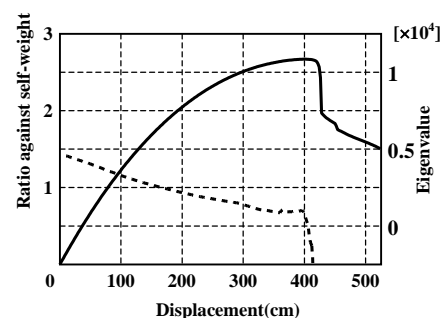


Figure 5: Load-displacement relationship at point B and changes in eigenvalue

maximum compressive stress is about 30 N/mm^2 . Tensile stress occurs at the arch springing, but it is only as small as several newtons per square millimeter, so the degree of safety from cracking is considered to be sufficiently high. It can be concluded, therefore, that cracking will not occur in the arch rib, and since the compressive stresses are within 1/3 of the compressive strength (i.e., within the elastic range), the performance requirements against concrete stress under normal loading are satisfied. The maximum steel stress occurring at the arch crown and the arch springing is about 160 N/mm^2 , which is smaller than 1/4 of the yield strength, indicating that the performance requirements are satisfied.

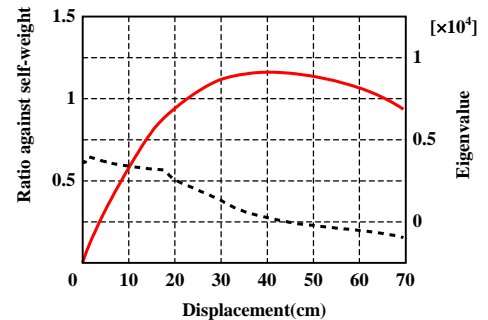
6 CHECK ON STABILITY UNDER SEISMIC LOADING

A verification model and an analysis method similar to the ones used for normal loading check were used for static and dynamic checks for seismic loading.

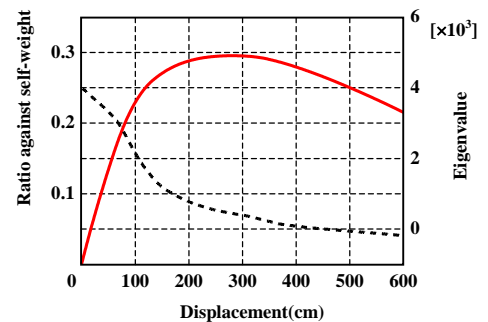
6.1 Static check

Static check was performed in the bridge axis direction and the direction perpendicular to the bridge axis. After the self-weight was applied, a load proportional to the dead load vector corresponding to each node in the verification model was applied under control in each direction to determine the load–displacement relationship. In addition, as in the normal loading check, the eigenvalue of the tangential stiffness matrix at each displacement step was considered.

Fig. 6 shows the load–displacement relationship at the top of the arch rib in the bridge axis direction and the direction perpendicular to the bridge axis (solid line) and changes in the eigenvalue of the tangential stiffness matrix (dotted line). In the bridge axis direction, the maximum load-carrying capacity was reached when the load was about 1.2 times the self-weight. In the direction perpendicular to the bridge axis, the load-carrying capacity was reached when the load was about 0.3 times the self-weight. In all cases, the eigenvalue of the first order of the tangential stiffness matrix gradually became smaller as deformation increased. In the bridge axis direction, the eigenvalue became zero when the maximum load was reached, while in the direction perpendicular to the bridge axis, the eigenvalue became zero after the maximum load was reached because of numerical errors. The continuity of eigenvalue changes indicates that the deformation mode on the basic path continued to occur after the maximum load was reached. These results indicate that the designed arch bridge is likely to show stable deformation behavior until the post-peak range



(a) Bridge axis direction



(b) Direction perpendicular to bridge

Figure 6: Load-displacement relationship and eigenvalue

without undergoing a sudden failure due to branching under static loads. It can be concluded, therefore, that the verification criteria for the structural stability (buckling safety) requirements under static loads are satisfied.

6.2 Dynamic check

In the dynamic check, the Newmark β method ($\beta=0.25$) was used for numerical integration in the time history response analysis. A damping ratio of 5% was used for all members. The "Inland, Type 1" and "Marine, Type 1" time history acceleration waveforms of Level 2 ground motions shown in Japan Society of Civil Engineers' Standard Specifications were used, and these ground motions were input at both of the fixed ends of the arch without taking phase difference into account. With respect to the input direction, three cases were considered: each of the time history acceleration waveforms was made to act (1) in the bridge axis direction, (2) in the direction perpendicular to the bridge axis or (3) in the bridge axis direction, the direction perpendicular to the bridge axis and the vertical direction at the same time. In the case of simultaneous input in the three directions, an identical waveform was let to act in the bridge axis direction and the direction perpendicular to the bridge axis direction, and a 1/2-acceleration waveform was let to act in the vertical direction.

a) Unidirectional input

Fig. 7 shows the time history response displacement at the top of the arch rib in the case where the "Inland, Type 1" time history acceleration waveform is input in the bridge axis direction and the case where the "Marine, Type 1" waveform is input in the same direction. Fig. 8 shows the time history response displacement in the cases where the same waveforms are input in the direction perpendicular to the bridge axis. In both figures, first-order eigenvalues of the tangential stiffness matrix at different times are shown with a dotted line. In calculating the eigenvalues of the tangential stiffness matrix, the tangential stiffness of the concrete after the maximum tensile stress was reached was regarded as zero in order to eliminate the influence of negative stiffness of concrete under tensile stress due to rapid decreases in stress.

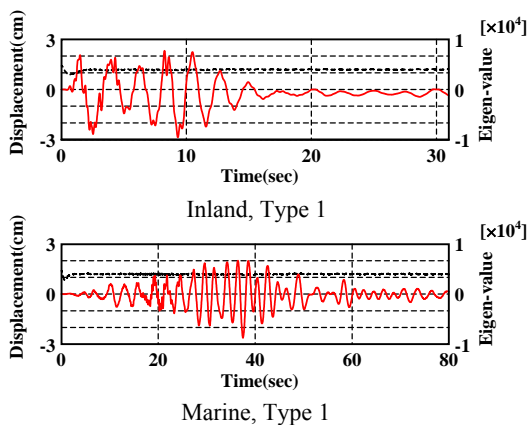


Figure 7: Response displacement in bridge axis direction and eigenvalue

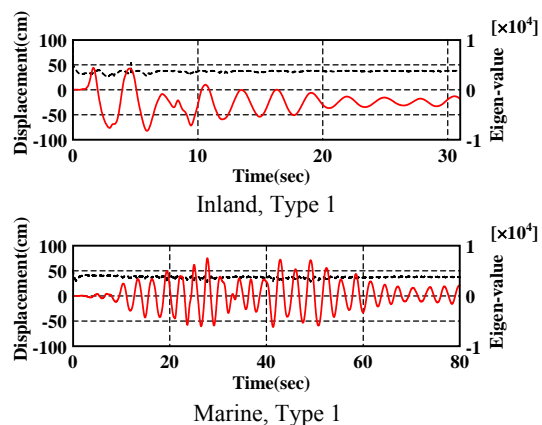


Figure 8: Response displacement in direction perpendicular to bridge axis and eigenvalue

The maximum response displacement in the bridge axis direction for both "Inland, Type 1" and "Marine, Type 1" waveforms is about 3 cm, which is considerably smaller than the displacement under the maximum static load of about 40 cm. The first-order eigenvalue of the tangential stiffness matrix did not become negative and varied very little during the response analysis. This means that the bridge is stable in the bridge axis direction against the input acceleration waveforms, and that the tangential stiffness matrix remained more or less unchanged because there occurred little nonlinear behavior. The maximum response displacement in the direction perpendicular to the bridge axis for both "Inland, Type 1" and "Marine, Type 1" waveforms was about 80 cm. This, too, is smaller than the displacement under the maximum static load of about 300 cm. The first-order eigenvalue of the tangential stiffness matrix did not become negative and remained more or less unchanged during the response analysis. In the case of the "Marine, Type 1" waveform input, however, response displacement became large again at input accelerations of 100 gal or less after the elapse of 40 seconds. The reason for this is thought to be that the dominant period of the acceleration waveform became longer after the elapse of 40 seconds, and it is necessary to pay attention to this. In any case, it is thought that the designed arch bridge is not likely to fail rapidly because of bifurcation under unidirectional earthquake loading and will be almost completely free from nonlinear behavior.

b) Simultaneous input in three directions

Fig. 9 shows the time history response displacement at the top of the arch rib in the case where the "Inland, Type 1" time history acceleration waveform is input in the bridge axis direction, the direction perpendicular to the bridge axis direction and the vertical direction (1/2 of the bridge axis direction and the direction perpendicular to the bridge axis) simultaneously. Fig. 10 shows the time history response displacement in the case where the "Marine, Type 1" time history acceleration waveform is similarly input in the three directions.

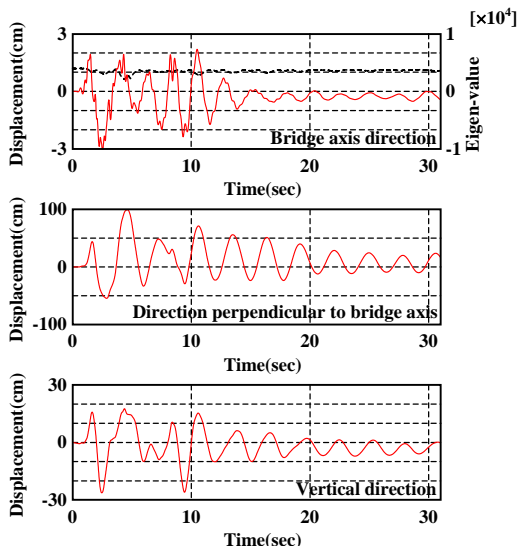


Figure 9: Response displacement and eigenvalue resulting from the "Inland, Type1" input

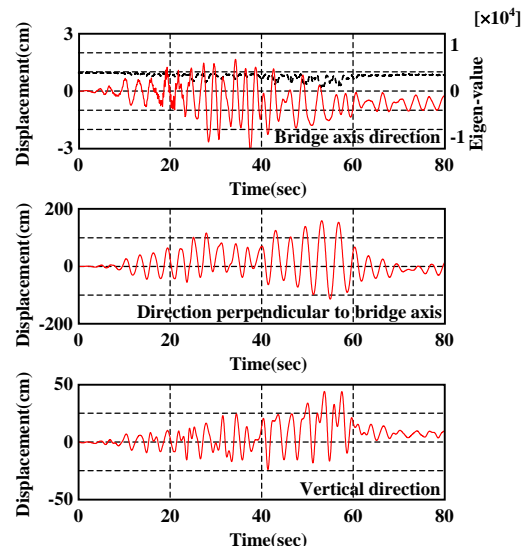


Figure 10: Response displacement and eigenvalue resulting from the "Marine, Type1" input

In the bridge axis direction graphs of Figs. 9 and 10, the first-order eigenvalues of the tangential stiffness matrix at different times are shown with dotted lines.

In the "Inland, Type 1" case, the maximum response displacement was about 3 cm in the bridge axis direction, about 100 cm in the direction perpendicular to the bridge axis, and about 25 cm in the vertical direction, all of which are considerably smaller than the displacements under the maximum loads during static loading. The first-order eigenvalue of the tangential stiffness matrix did not become negative and varied very little during the response analysis. In the "Marine, Type 1" case, the maximum response displacement was about 3 cm in the bridge axis direction, about 150 cm in the direction perpendicular to the bridge axis, and about 40 cm in the vertical direction. Thus, the displacement in the direction perpendicular to the bridge axis in the "Marine, Type 1" case was greater than that in the "Inland, Type 1" case. The first-order eigenvalue of the tangential stiffness matrix decreased about the time the displacement in the direction perpendicular to the bridge axis was maximized. From this, it can be inferred that the range showing nonlinear behavior was reached. The amount of displacement, however, was only about half the amount of displacement under the maximum load during static loading. Another characteristic is that as in the case of unidirectional input, response displacement in the direction perpendicular to the bridge axis is maximized after the elapse of 40 seconds, when the input acceleration was smaller than 100 gal.

From these results, it can be concluded that the designed arch bridge has sufficient seismic performance and is sufficiently safe against seismically induced buckling.

7 CONCLUSION

The findings of the studies conducted on the trial design of a long-span concrete arch bridge can be summarized as follows:

- It is possible to find appropriate sites for arch-under-deck, long-span concrete arch bridges in Japan if a low-rise arch design is adopted.
- In the case of a flat arch with an arch span of 500 m and an arch rise of 40 m, the design strength of arch rib concrete must be at least 100 to 120 MPa.
- It has been confirmed that even such a flat-arch bridge has sufficient structural stability under normal and earthquake loading.
- The construction period of a marine bridge can be shortened by lifting a pre-assembled Melan arch into place from a floating platform.

REFERENCES

- [] S. Orita, H. Fukuda, T. Maeda, H. Fujioka, K. Kamisakoda and S. Sano: "Construction of Ikara Bridge superstructure" (in Japanese), *Bridge and Foundation Engineering*, Vol. 29, No. 11, pp. 7–14, 1995.
- [] H. Nakamura, J. Niwa and T. Tanabe: "Analytical study on the ultimate deformation of RC columns" (in Japanese), *Proceedings of JSCE*, No. 420/V-30, pp. 115–124, 1990.
- [] JSCE: *Standard specifications for design and construction of concrete structures: verification of seismic performance* (in Japanese), Japan Society of Civil Engineers, 2002.